Chapter 2

High Temperature Hyperthermia in Breast Cancer Treatment

Mario Francisco Jesús Cepeda Rubio,
Arturo Vera Hernández and Lorenzo Leija Salas

Additional information is available at the end of the chapter

http://dx.doi.org/10.5772/53277

1. Introduction

Globally, breast cancer is the most common type of cancer among women, which comprises 23% of all female cancers that are newly diagnosed in more than 1.1 million women each year. Over 411 000 deaths result from breast cancer annually; this accounts for over 1.6% of female deaths from all causes. Hyperthermia also called thermal therapy or thermotherapy is a type of cancer treatment in which body tissue is exposed to high temperatures. Research has shown that high temperatures can damage and kill cancer cells, usually with minimal injury to normal tissues. Otherwise, ablation or high temperature hyperthermia is defined as the direct application of chemical or thermal therapies to a tumor to achieve eradication or substantial tumor destruction. Many ablation modalities have been used, including cryoablation, ethanol ablation, laser ablation, and radiofrequency ablation. The most recent development has been the use of microwave ablation in tumors. Furthermore, The use of breast cancer mammography screening has allowed detecting a greater number of small carcinomas and this has facilitated treatment by minimally invasive techniques. Currently, physicians test minimally invasive ablation techniques to determine if they will be acceptable substitutes for surgical removal of primary breast tumors. Therefore, numerical electromagnetic and thermal simulations are used to optimize the antenna design and predict heating patterns. A review of different hyperthermia ablative therapies, for breast cancer treatment is summarized in this work. Otherwise, advanced computer modeling in high hyperthermia treatment and experimental model validation will be referred to in this chapter.

1.1. Tumor ablation

Tumor ablation is defined as the direct application of chemical or thermal therapies to a tumor to achieve eradication or substantial tumor destruction. The aim of tumor ablation is

to destroy an entire tumor by using heat to kill the malignant cells in a minimally invasive fashion together with a sufficient margin of healthy tissue, to prevent local recurrence. Many ablation modalities have been used, including cryoablation, ethanol ablation, laser ablation, and radiofrequency ablation (RFA). The most recent development has been the use of microwave ablation (MWA) in tumors [1].

Nevertheless the local application of heat to treat patients with malignant tumors is not a novel concept. The Edwin Smith papyrus describes the topical application of hot oil or heated metallic implements that were used approximately 5000 years ago to treat patients with tumors [2]. The use of an electrical current to produce thermal tissue necrosis in patients with breast carcinoma also is not new: Metallic or clay-insulated electrodes were inserted into locally advanced breast tumors in the late 19th century to shrink the tumor and reduce pain and bleeding [3].

1.2. Principles of tissue damage

1.2.1. Radiofrequency ablation

This therapy works by converting radiofrequency waves into heat through ionic vibration. Alternating current passing from an electrode into the surrounding tissue causes ions to vibrate in an attempt to follow the change in the direction of the rapidly alternating current. It is the ionic friction that generates the heat within the tissue and not the electrode itself. The higher the current, the more vigorous the motion of the ions and the higher the temperature reached over a certain time, eventually leading to coagulation necrosis and cell death. The ability to efficiently and predictably create an ablation is based on the energy balance between the heat conduction of localized radiofrequency energy and the heat convection from the circulation of blood, lymph, or extra and intracellular fluid [4]. The amount of radiofrequency produced heat is directly related to the current density dropping precipitously away from the electrodes, thus resulting in lower periphery temperatures. It can be approximated that the heat generated in a region at distance d from the electrode drops as 1/d4. The goal of radiofrequency ablation is to achieve local temperatures that are lethal to the targeted tissue. Generally, thermal damage to cells begins at 42°C; and once above 60°C, intracellular proteins are denatured, the lipid bilayer melts, and irreversible cell death occurs [5].

1.2.2. Microwave ablation

Water molecules are polar, that is, the electric charges on the molecules are asymmetric. The alignment and the charges on the atoms are such that the hydrogen side of the molecule has a positive charge, and the oxygen side has a negative charge. When an oscillating electric charge from radiation interacts with a water molecule, it causes the molecule to flip. Microwave radiation is specially tuned to the natural frequency of water molecules to maximize this interaction. Temperature is a measure of how fast molecules move in a substance, and the vigorous movement of water molecules raises the temperature of water.

Therefore, electromagnetic microwaves heat matter by agitating water molecules in the surrounding tissue, producing friction and heat, thus inducing cellular death via coagulation necrosis [6].

1.3. Ablative devices

1.3.1. Radiofrequency ablation

The different manufacturers employed various strategies to obtain larger ablation zones [7]; there are currently three different manufacturers that offer commercial radiofrequency tumor ablation devices in the USA (Boston Scientific, Rita Medical and Valleylab) and an additional one in Europe (Celon). Two manufacturers (Boston Scientific and Rita Medical) employ multitined electrodes, to increase electrode surface area and volume of tissue heating. For multitined electrodes typically an incremental deployment of the tines in stages is used, with ablation at each deployment stage for a certain amount of time or until the target temperature is achieved to ensure complete ablation of the target volume. Two manufacturers use internal electrode cooling via circulation of water or saline to increase ablation zone size (Valleylab and Celon). By cooling the electrode, the tissue surrounding the electrode is also cooled. The location of maximum temperature is 'pushed' further into the tissue, resulting in a larger ablation zone size. A similar effect is obtained by infusing saline into the tissue via ports in the electrode this method is used by the Starburst Xli™ electrode [8].

1.3.2. Microwave ablation

A variety of probes have been proposed for use in MWA, with the majority being based on a coaxial structure due to the deep-seated location of many tumors and the angular symmetry of the tumor. Initial antennas based upon a coaxial waveguide structure include designs, such as the monopole, dipole and slot antennas, often encased in a polytetrafluoroethylene (PTFE) catheter to minimize adhesion of the probe to desiccated ablated tissue. A number of challenges, characteristics and trade-offs have been identified in the design of MWA probes. Challenges include the reduction of backward heating, minimization of probe diameter and impedance matching of the antenna to the surrounding tissue. Trade-offs in design involve probe diameter versus maximum application of power and ablation power versus ablation time. Early coaxial antennas developed for MWA yielded ablation zones resembling a 'tear drop', as opposed to the desired spherical shape [9]. More recent MWA probes were designed to minimize probe size, maximize ablation zone size, minimize detrimental heating of the feedline and yield more spherical lesions, by minimizing impedance mismatch [10-12].

2. Clinical applications

2.1. Radiofrequency ablation

The first RFA clinical report was published in 1999, Jeffrey *et al.* [13] treated with RFA a small series of five women, aged 38 to 66 years, with locally advanced (stage III) breast

cancer or tumors larger than 5 cm. While patients were under general anesthesia and just before surgical resection, a 15-gauge insulated multiple-needle electrode (LeVeen needle electrode; RadioTherapeutics Corp, Mountain View, Calif) was inserted into the tumor under sonographic guidance. The multiple-needle electrode was connected to a RF-2000 generator (Radio Therapeutics Corp), and a return electrode pad (Valley Lab, Boulder, Colo). Radiofrequency energy was applied at a low power by a preset protocol for a period of up to 30 minutes. The ablated area measured 0.8–1.8 cm diameter and non-viable tumor was found within this area in four patients.

Izzo *et al.* [14] used the same RFA electrode in patients with much smaller tumours. Twenty-six women with a mean cancer size of 18 mm underwent RFA and immediate surgical excision. RFA was performed following a predetermined two-phase algorithm. Treatment was initiated at 10 watts of power for 2 minutes, after which, power was increased in 5-watt increments every minute until tissue impedance rose rapidly and power dropped below 10 watts, thus indicating complete coagulative necrosis of the target lesion. After a 30-second pause, a second phase of treatment was applied, again beginning at 10 watts for 2 minutes followed by increases in power of 5 watts per minute until tissue impedance again rose and power rolled off. Power (watts) and impedance (ohms) were monitored continuously during treatment. The maximum power at the time of increase in the tissue impedance preceding power roll off and the total time needed to complete two-phase RFA were recorded. NADH diaphorase histochemical analysis showed a residual cancer focus in an area adjacent to the needle shaft site in one case, while the remaining patients were treated successfully with a complication rate of 4%.

Burak *et al.* [15] treated tumours with a mean diameter of 12 mm, creating an ablation zone of 26–45 mm and reported one case with surviving malignancy. Viability was assessed using cytokeratin 8/18 stain. Under ultrasound guidance, 1% lidocaine was injected around the breast tumor for a distance of about 3 cm in all directions surrounding the tumor mass. After a 5–10-minute waiting period, a small skin incision was made with a number 11 surgical blade under aseptic conditions. The 2 cm array RFA probe (Radiotherapeutics, Sunnyvale, CA) was inserted under ultrasound guidance and deployed so that the "prongs" encompassed the breast tumor. Radiofrequency energy was applied over 2 time periods, which were not to exceed a total of 30 minutes. In the first time period, power was set to 10 W and increased in 5 W intervals every 2 minutes until a rapid increase in impedance (ohms) occurred, or when 60 W was reached. If 60 W was obtained, the probe was left in place until impedance or a total period of 15 minutes elapsed. In the second time period, the application began at 10W and the same titration was followed.

Hayashi *et al.* [16] ablated small breast primaries measuring 9 mm median in 22 patients. The median ablated diameter was 35 mm, viability was assessed with NADHdiaphorase and showed eight failures. In three, the site was at the periphery but in five was in a missed untargeted area. Under sterile conditions in the ultrasonography suite, a 15-gauge, 7-array StarBurst radioprobe (RITA Medical Systems, Mountain View, California) was placed directly into the tumor using sonographic guidance (HDI 3000; Phillips Medical, Bothell,

Washington). The prongs were deployed after positioning was confirmed in three dimensions using real-time ultrasound. The probe was connected to the RF generator (RITA model 1500) with a grounding pad placed on each thigh to complete the electrical circuit. The generator was set to automatic, power at 20 W, temperature to 95°C, and ablation time set at 15 minutes. The generator was activated and power was delivered incrementally until the target temperature was attained and held for the set time. The ablation process was monitored with ultrasonography and real time temperature feedback. Vital signs were monitored and if the patient reported significant discomfort, the ablation was temporarily halted. On completion of the procedure, the tines were retracted and the needle withdrawn.

Fornage *et al.* [17] treated 21 breast tumours of < 2 cm and in the subsequent excision specimen all targeted cancer foci were ablated with an average diameter of 3.8 cm. One patient who had received neoadjuvant chemotherapy was found to have a further mammographically and ultrasonically occult viable tumour. A 460-kHz monopolar RF electrosurgical generator specifically designed for use with electrosurgical RF probes (RITA Medical Systems, Mountain View, Calif) was used in this study. The needle-electrode consists of a primary electrode— that is, a 15-gauge stainless-steel cannula with a noninsulated distal tip that acts as an electrode—and secondary electrodes, which are curved, flexible stainless-steel prongs that are contained within and can be deployed outside of the primary electrode. A 50-W model 500 electrosurgical RF generator (RITA Medical Systems) with a disposable, seven-array model 70 Starburst needle electrode (RITA Medical Systems) was used in the first nine patients. Subsequently, a 150-W model 1500 generator (RITA Medical Systems) with a nine-array Starburst XL needle-electrode (RITA Medical Systems) was used in 11 patients. Both types of needle-electrodes were 15 cm long. The arrays on the Starburst XL needle-electrode can be deployed to a length of 5 cm. Thermocouples placed at the tips of four prongs of the seven-array needleelectrode and at the tips of five prongs of the nine-array needle-electrode enabled continuous real-time monitoring of the temperatures at the tips. A laptop computer with proprietary software developed by the manufacturer of the RF ablation equipment was used to graphically display, in real time, the curves of the temperatures at the tips, the power of the generator, and the impedance of the tissues over time.

Marcy *et al.* [18] treated five cancers in four not-fit-for-surgery patients with RFA and had one relapse after 4 months. Percutaneous radiofrequency–lumpectomy was performed under local analgesia (lidocaine, subcutaneous injection), using ultrasound guidance under sterile conditions in the interventional radiology suite. RFA was applied between a large neutral electrode, leading to a high electric field line density in the region of the needle tip, and the 1.5 mm x 1.1 mm non-isolated needle tip ablation electrode. Thermal lesions were always produced with RF power 30 W, at a frequency of 500 kHz, during a 12 min application time as recommended by the manufacturer (Elektrotom 104HF; Thermo-Berchtold Medizinelektronik Gmbh, Tuttlingen, Germany). A controlled interstitial needle perfusion of isotonic sterile saline solution (0.9% NaCl) was applied using an infusion pump (Perfusor Secura FT; Braun, France). The current flows from the uninsulated perfused electrode implanted in the tumour to a grounding pad applied externally to the skin. A

feedback system controlling RF power application and saline infusion of the needle maintains power delivery. The RFA probe was designed to create a minimum spherical ablation volume of 3 cm diameter. Thermocoagulation included the tumour plus at least a 5 mm margin. The RFA probe was typically positioned parallel to the overlying skin under ultrasound guidance, and the procedure was carried out during real-time ultrasound monitoring. Ablation zones were visualized as cone-shaped hyperechogenic areas around the needle tip, experiencing the temperature increase. Vital signs were monitored and if the patient reported significant discomfort, the ablation was temporarily halted. On completion of the procedure, the lines were retracted and the needle withdrawn. A small ice pack was placed on the wound for up to 24 h after the procedure for comfort. The patient was discharged home once stable and free of sedative effects.

Susini *et al.* [19] treated three patients who had small breast cancers with RFA and followed them with clinical examination, ultrasound, magnetic resonance imaging (MRI) and core biopsy. After 18 months no relapses were reported. The 18-G Cool tip RF Radionics (Valley Lab, USA) was used to perform RFA, by means of one single electrode, 20-cm length. Local anesthesia was performed using a mixture of lidocaine and naropine injected under the overlying skin, and around the tumor. With ultrasound guidance, the electrode was inserted and its progression was monitored in real-time, allowing the exact positioning of the tip in the center of the lesion. Then, the RF generator was switched on and tissue impedance was measured. The generator produced RF energy through high-frequency (480 kHz) alternating current. When the tissue temperature reached 90°C, ultrasound image showed the "fog effect", in relationship with the vaporization of intracellular water. RF energy was applied for a variable time of 8–12 min.

Oura *et al.* [20] in their series of 52 patients with breast cancers of mean size 1.3 cm. Multifocality, multicentricity and tumour size were thoroughly investigated prior to RFA and patients with multiple malignant areas or large tumours were excluded. Patients were submitted to ultrasound guided RFA and were subsequently followed with clinical examination, ultrasound, MRI and cytology. After a mean follow-up of 18 months no relapses were reported. Operation was performed under general anesthesia in all patients. After the removal of sentinel node(s), RFA started using a Cool-tip RF needle with an uninsulated tip 3 cm in diameter (Valleylab, Boulder, CO). The Cool-tip RF needle was inserted into the tumor from the areola under ultrasound guidance. A total of 20-60 mL of 5% glucose was injected subcutaneously just above the tumor after appropriate insertion of the needle was confirmed. The RFA started at 5 watts, raised the output to 10 watts 1 minute later, and thereafter increased output continuously in increments of 10 watts at 1 minute intervals until either the generator stopped delivering radiofrequency energy due to a 20 ohms or more impedance increase of the ablated tissue from the base line, or the scheduled time which was 30 minutes in the first 29 cases and 15 minutes thereafter when'break'did not occur.

Medina *et al.* (2008) [21] treated Twenty-five patients, aged 42 to 89 years with invasive breast cancer <4 cm (range 0.9–3.8 cm). Under ultrasound guidance, a 17-gauge probe

(Elektrotom 106 HiTT, Berchtold, Germany) was inserted in the center of the tumor. The needle electrode was attached to a 500 kHz monopolar RFA generator. RF energy was applied to the tissue with initial power setting of 30 W, for three cycles of 3 minutes each. The energy was increased with increments of 5 W to a maximum power of 50 W. Radiofrequency was delivered until the tumor was completely hyperechoic with the aim of obtaining a safety margin of 1 cm around the tumor. Of the 25 patients treated, NADPH stain showed no evidence of viable malignant cells in 19 patients (76%), with significant difference between tumors <2 cm (complete necrosis in 13 of 14 cases, 92.8%).

Currently Takayuki [22] *et al.* treated 49 patients, aged 36 – 82 years and tumor size ≤3.0 cm in diameter (range 0.5–3.0 cm) on US examination. Under US guidance, the 17-gauge ValleylabTM RF Ablation System with Cool-tip™ Technology (Covidien, Energy-Based Devices, Interventional Oncology, Boulder, CO) was inserted in the center of the tumor. The needle electrode was attached to a 500-kHz monopolar RF generator capable of producing 200-W power. Tissue impedance was monitored continuously using circuitry incorporated into the generator. RF energy was applied to tissue with an initial power setting of 10 W and subsequently increased with increments of 5 W each minute to a maximum power of 55 W. The power setting was left at this point until power 'rolloff' occurred. Power rolloff implies that there is an increase in the tissue impedance. When this occurs, the power generator will shut off, stopping the flow of current and further tissue coagulation. After waiting 30–60 s, the second phase was started at 75% of the last maximum power until a second rolloff occured. Radiofrequency was applied until the tumor was completely hyperechoic. Following RF ablation, standard tumor resection was achieved with either a wide local excision or mastectomy according to the preference of the patient. Of the 49 treated patients, complete ablation was recognized in 30 patients (61%) by H&E staining and/or NADH diaphorase staining. A summary is presented in tables 1-4.

Authors	Patients	Age range	Tumor Size (cm)
Jeffrey	5	38-66	4-7
Izzo	26	37-78	0.7-3.0
Burak	10	37-67	0.5-2.0
Hayashi	22	60-80	0.5–2.2
Fornage	20	38-80	≤2.0
Marcy	4	79-82	1.8-2.3
Susini	3	76-86	<2.0
Oura	52	37-83	0.5-2.0
Medina	25	42-89	0.9 - 3.8
Takayuki	49	20-90	≤3.0

Table 1. Patient and tumor characteristics in ten studies on radiofrequency ablation for breast cancer

Authors	Electrode Probe	Generator
Jeffrey	15-g multineedle LeVeen	RF-2000 Radio Therapeutics
Izzo	15-g multineedle LeVeen	RF-2000 Radio Therapeutics
Burak	2 cm array probe Radio therapeutics	Not mentioned
Hayashi	15-g, 7 cm array Starburst RITA	RITA-1500 RITA
Fornage	7-array / 15-g, 9 cm array Starburst RITA	RITA-500 / RITA-1500
Marcy	1.5 mm · 1.1 mm non-isolated tip Elektrotom	Elektrotom 104HF
Susini	18-G Cool tip RF Radionics	Not mentioned
Oura	3 cm Cool-tip uninsulated Valleylab	Not mentioned
Medina	17-g Elektrotom 106, Germany	Monopolar 200 W
Takayuki	17-g Valleylab RF Ablation System with Cool-tip	Monopolar 200 W

Table 2. Devices in ten studies on radiofrequency ablation for breast cancer

Authors	Frequency	Feedback control	Temperature (ºC)	Image guided
Jeffrey	480-kHz	Impedance	46.8 - 70.0	Ultrasound
Izzo	480-kHz	Impedance	Not mentioned	Ultrasound
Burak	460 kHz	Impedance	Not mentioned	Ultrasound
Hayashi	460 KHz	NO	95	Ultrasound & Doppler
Fornage	461 KHz	NO	90 and 95	
Marcy	500 kHz	NO	Not mentioned	Ultrasound
Susini	480 kHz	NO	90	Ultrasound
Oura	Not mentioned	Impedance	> 60	Ultrasound
Medina	500 KHz	NO	70 - 80	Ultrasound
Takayuki	500 KHz	Impedance	Not mentioned	Ultrasound

Table 3. Technical settings in ten studies on radiofrequency ablation for breast cancer

Authors	Anesthesia	Fail	Complications
Jeffrey	General	1	0
Izzo	General	1	1
Burak	Local	1	1
Hayashi	Local	3	1
Fornage	General	1	0
Marcy	Local	1	0
Susini	Local	0	0
Oura	General	0	1
Medina	General	6	1
Takayuki	General	18	5

Table 4. Results in ten studies on radiofrequency ablation for breast cancer

2.2. Microwave ablation

Three studies on microwave ablation have been published [23-25]. A pilot safety (phase I) study included ten patients with core needle biopsy-proven invasive breast carcinoma (T1–T3 tumors) [23]. Of the eight patients who responded, 82–97% tumor cell kill was found, confirmed by M30 immunohistochemistry. Image guidance was performed using US. Five to 27 days after treatment patients underwent mastectomy. The same group also published another article in which 21 patients with T1–T2 invasive breast carcinoma underwent microwave ablation [24]. In 68% of the patients, histologic evidence of tumor necrosis was present. Finally, this group published a dose-escalation study [25].

Twenty-five patients with core needle biopsy-proven invasive breast carcinoma (T1–T2 tumors) were included. US provided image guidance; there was no correlation between clinical/ultrasonographic size changes and pathologic tumor response. In 68% of the cases there was evidence of pathologic response using H&E staining. In two cases complete ablation was reached; these patients received the highest temperature dose. Complications mentioned were mild pain during treatment, skin burn, and short-lived erythema of the skin.

2.3. Summary

In RFA several different devices from different manufacturers were used in different ways for varying periods of time and varied protocols, so not surprisingly, they reported quite heterogeneous results. Nevertheless successful cases for different protocols were obtained for smaller tumors with a low failures and complication rate. In addition the clinical MWA is limited to external techniques and currently the greatest amount of interstitial research was conducted in the liver tissue. The generation of an appropriately sized ablation zone, long treatment times, insufficient interoperative imaging modalities and performance in the

vicinity of vascular structures are limitations of current devices. An ideal ablative technology would ensure complete destruction of all malignant cells with no significant side effects or complications.

3. Advanced computer modeling in breast cancer hyperthermia treatment

In this section, we present a computer modeling for microwave high hyperthermia in breast cancer treatment. Computational electromagnetic (CEM) or electromagnetic modeling employs numerical methods to describe propagation of electromagnetic waves. It typically involves the formulation of discrete solutions using computationally efficient approximations to Maxwell's equations. There are three techniques of CEM: the finite-difference time-domain (FDTD), the method of moments (MOM), and the finite element method (FEM), which has been extensively used in simulations of cardiac and hepatic radiofrequency (RF) ablation [26]. A FEM model was used in this work because it can provide users with quick, accurate solutions to multiple systems of differential equations and therefore, they are well suited to solve heat transfer problems like ablation [27]. Numerous MWA antenna designs specifically targeted for MWA cardiac and hepatic applications have been reported [20-24], but they have not been used to treat breast cancer. These designs have been focused largely on thin, coaxial-based interstitial antennas [28], which are minimally invasive and capable of delivering a large amount of electromagnetic power. These antennas can usually be classified as one of three types (dipole, slot, or monopole) based on their physical features and radiation properties [29]. On the other hand, several researchers are investigating non-invasive microwave hyperthermia for treatment of breast cancer [30].

3.1. Equations

The frequency-dependent reflection coefficient can be expressed logarithmically as:

$$\Gamma(f) = 10 \cdot \log_{10}\left(\frac{P_r(f)}{P_{in}}\right)[dB] \tag{1}$$

where, Pin is the input power and Pr indicates the reflected power (W). SAR represents the amount of time average power deposited per unit mass of tissue (W/kg) at any position. It can be expressed mathematically as:

$$SAR = \frac{\sigma}{\rho}\left|E\right|^2 = \left[W / Kg\right] \tag{2}$$

where, σ is tissue conductivity (S/m), ϱ is tissue density (kg/m^3) and E is the electric field [56]. The SAR takes a value proportional to the square of the electric field generated around the antenna and is equivalent to the heating source created by the electric field in the tissue. The SAR pattern of an antenna causes the tissue temperature to rise, but does not determine the final tissue temperature distribution directly. The tissue temperature increment results

from both power and time. MW heating thermal effects can be roughly described by Pennes' Bioheat equation [31]:

$$\nabla \cdot (-k\nabla T) = \rho_b C_b \omega_b (T_b - T) + Q_{met} + Q_{ext} \quad (3)$$

where k is the tissue thermal conductivity (W/m°K), ϱ_b is the blood density (Kg/m^3), C_b is the blood specific heat (J/Kg°K), ω_b is the blood perfusion rate (1/s). Tb is the temperature of the blood and T is the final temperature. Q_{met} is the heat source from metabolism and Q_{ext} an external heat source. The major physical phenomena considered in the equation are microwave heating and tissue heat conduction. The temperature of the blood is approximated as the core temperature of the body. Moreover, in ex vivo samples, ω_b and Q_{met} can be neglected since no perfusion or metabolism exists. The external heat source is equal to the resistive heat generated by the electromagnetic field.

3.2. Material properties

The computer antenna model used in this work is based on a 50Ω UT-085 semirigid coaxial cable. The entire outer conductor is copper, in which a small ring slot of width is cut close to the short-circuited distal tip of the antenna to allow electromagnetic wave propagation into the tissue. The inner conductor is made from silver-plated copper wire (SPCW) and the coaxial dielectric is a low-loss polytetrafluoroethylene (PTFE). The length of the antenna also affects the power reflection and shape of the SAR pattern. Furthermore, the antenna is encased in a PTFE catheter to prevent adhesion of the antenna to desiccated ablated tissue. Dimensions and thermal properties of the materials and breast tissue, which were taken from the literature [32], are listed in Table 5 and 6.

Parameter	Value
Center conductor diameter	0.51 mm
Dielectric diameter	1.68 mm
Outer conductor diameter	2.20 mm
Diameter of catheter	2.58 mm
Power	10 W
Frequency	2.45 GHz
Electrical Conductivity of breast	0.137 S/m
Thermal conductivity of breast	0.42 W/m K
Specific heat of blood	3639 J/Kg/k
Blood perfusion rate	0.0036 s-1
Electrical conductivity of tumor	3 S/m
Thermal conductivity of tumor	0.5 W/m K

Table 5. Dimensions and properties for the materials and tissue.

Material	Relative permittivity
Inner dielectric oft he coaxial cable	2.03
Catheter	2.60
Breast tissue	5.14
Tumor	57

Table 6. Relative permittivity for the materials and tissue.

Figure 1 shows the axial schematics of each section of the antenna and the interior diameters.

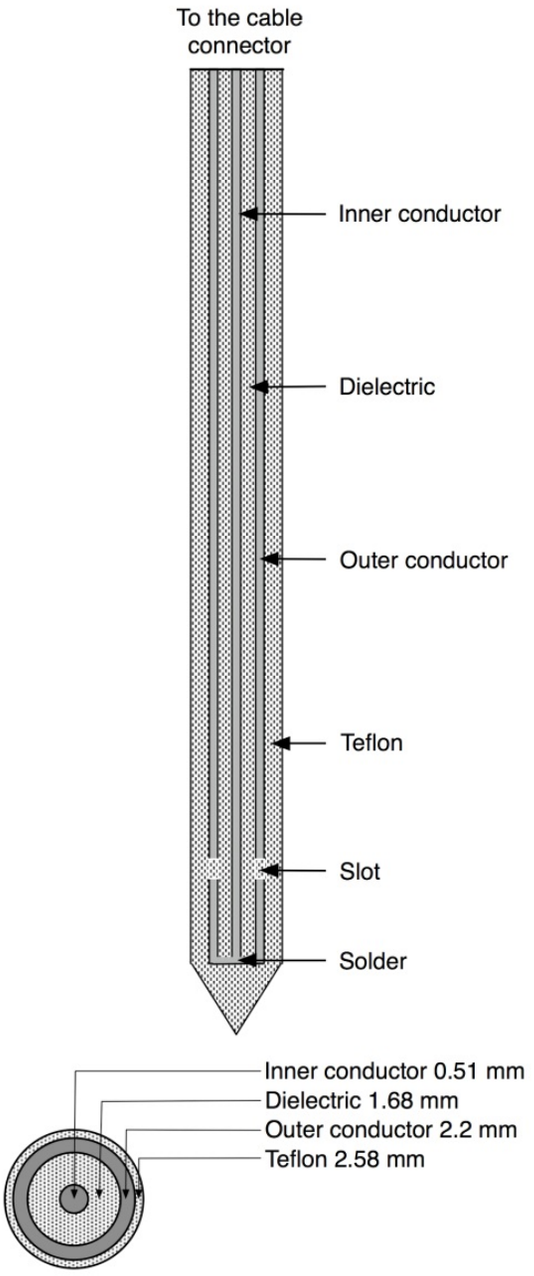

Figure 1. Cross section and axial schematic of the coaxial slot antenna.

A finite element method computer models were developed using COMSOL Multiphysics 4.0 commercial software. One of the models assumed that the coaxial slot antenna was immersed only in homogeneous breast tissue; the other model assumed that the antenna was immersed only in breast cancer. The coaxial slot antenna exhibits rotational symmetry around the longitudinal axis; therefore axisymmetric models, which minimized the computation time, were used. The inner and outer conductors of the antenna were modeled using perfect electric conductor boundary conditions and boundaries along the z axis were set with axial symmetry.

All boundaries of conductors were set to perfect electric conductor (PEC). Boundaries along the *z* axis were set with axial symmetry and all other boundaries were set to low reflection boundaries. Figure 2 shows the geometry of the antenna model with details near its slot; since the model is axisymmetric, only a half of the antenna geometry structure is shown [33].

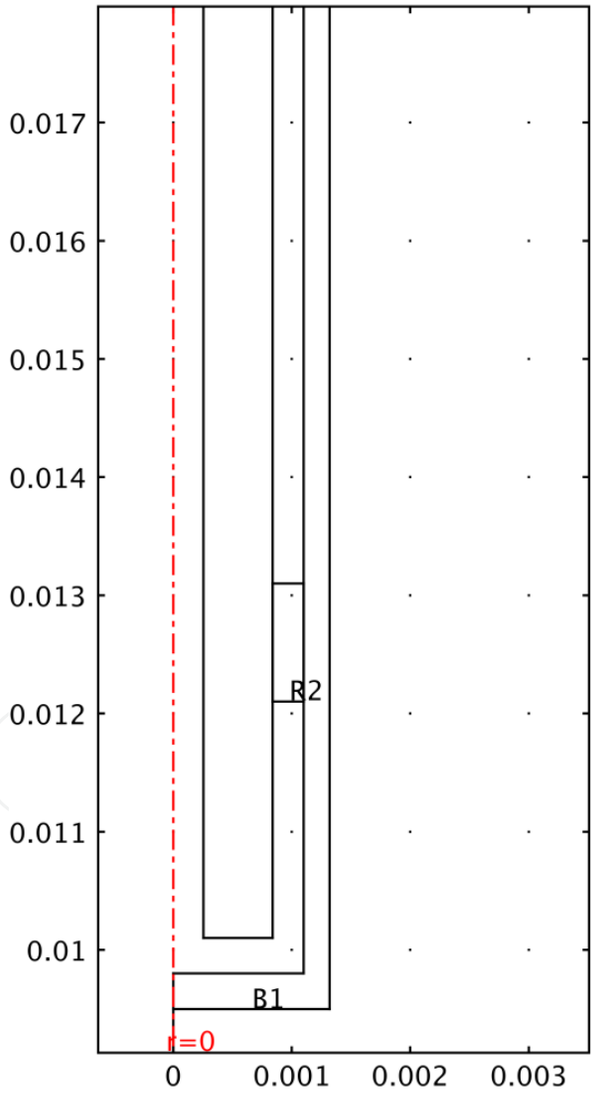

Figure 2. Axisymmetric model in the vicinity of the tip of the coaxial slot antenna. The vertical axis (z) corresponds to the longitudinal axis of the antenna; while the horizontal axis (r) corresponds to radial direction. All units are in meters.

3.3. Results

Figure 3 shows the temperature distribution in normal adipose-dominated tissue [34]. The reflection coefficient calculated for the frequency at 2.45 GHz was -2.82 dB, the maximum temperature was 116.03 ºC, and the ablation zone radius was 53 mm. The isotherm was considered at 60 ºC because ablation is produced above this temperature [35]. Figure 4 shows the temperature distribution in breast cancer tissue. The reflection coefficient calculated for the frequency at 2.45 GHz was -6.38 dB, the maximum temperature was 125.96 ºC, and the ablation zone radius was 92 mm.

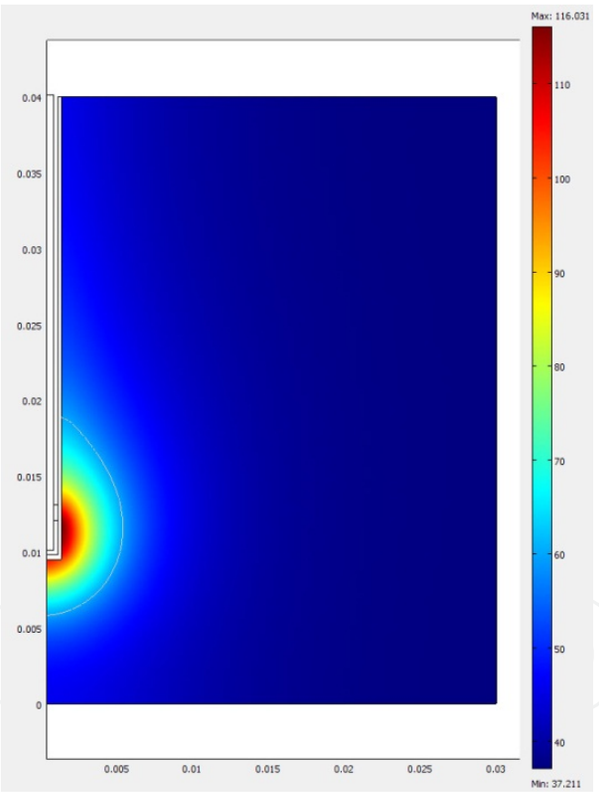

Figure 3. Temperature distribution of normal adipose-dominated breast tissue at a microwave power output of 10 W. The isotherm at 60 ºC is highlighted. The illustration shows half the plane through the symmetry axis. Vertical axis (z) corresponds to the longitudinal axis of the antenna; horizontal axis (r) corresponds to radial direction.

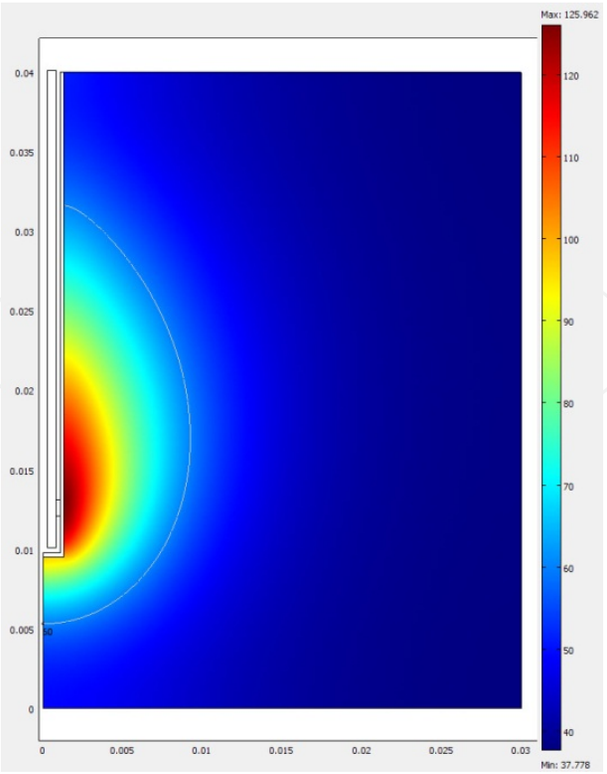

Figure 4. Temperature distribution of breast cancer tissue at a microwave power output of 10 W. The isotherm at 60 ºC is highlighted. The illustration shows half the plane through the symmetry axis. Vertical axis (z) corresponds to the longitudinal axis of the antenna; horizontal axis (r) corresponds to radial direction.

4. Conclusion

In RFA for high temperature hyperthermia therapy in breast cancer several devices from different manufacturers were used in diverse ways for varying periods of time and assorted protocols, therefore exist heterogeneous results. Nevertheless successful cases for were obtained for smaller tumors with a low failures and complication rate. On the other hand the effect of MWA on malignant and normal adipose-dominated tissues of the breast was simulated using an axisymmetric electromagnetic model. This model can analyze the heating patterns using the bioheat equation. The results from computer modeling demonstrated that, effectively, the difference in dielectrical properties and thermal parameters between the malign and normal adipose-dominated tissue could cause the preferential heating on tumor during MWA. Even though electromagnetic high temperature hyperthermia requires further research, it is a promising minimally invasive modality for the local treatment of breast cancer.

Acknowledgement

The project described was supported by Instituto de Ciencia y Tecnología del Distrito Federal. Project Name: "Desarrollo de un sistema automatizado de determinación

volumétrica por imágenes ultrasónicas para cuantificar el efecto de la energía térmica aplicada en la ablación del cáncer. Number: PICCO10-78. Agreement: ICYTDF; 340/2010.

Author details

Mario Francisco Jesús Cepeda Rubio,
California State University, Long Beach & Instituto de Ciencia y Tecnología del Distrito Federal (ICyTDF)

Arturo Vera Hernández and Lorenzo Leija Salas
Centro de Investigación y de Estudios Avanzados del Instituto Politécnico Nacional, Department of Electrical Engineering/Bioelectronics, Mexico

5. References

[1] Berber E, Flesher NL, Siperstein AE. Initial clinical evaluation of the RITA 5-centimeter radiofrequency thermal ablation catheter in the treatment of liver tumors. The Cancer Journal 2000; 6:319–329.

[2] Breasted JH. The Edwin Smith surgical papyrus, vol. 54. Chicago: Chicago University Press; 1930.

[3] Rockwell AD. Electro-surgery: benign and malignant tumors. In: Rockwell AD, editor. The medical and surgical uses of electricity. New York: EB Treat & Company 1903; 565–6.

[4] Scudamore C. Volumetric radiofrequency ablation: technical consideration. The Cancer Journal 2000; 6:316–318.

[5] C. J. Simon, D. E. Dupuy, and W. W. Mayo-Smith. Microwave Ablation: Principles and Applications. RadioGraphics 2005; 25(suppl_1): S69 - S83.

[6] Goldberg SN, Gazelle GS. Radiofrequency tissue ablation: physical principles and techniques for increasing coagulation necrosis. Hepatogastroenterology 2001; 48(38), 359–367.

[7] Lobik L, Leveillee RJ, Hoey MF. Geometry and temperature distribution during radiofrequency tissue ablation: an experimental ex vivo model. J. Endourol. 2005; 19(2), 242–247.

[8] O'Rourke, Ann P; Haemmerich, Dieter; Prakash, Punit; Converse, Mark C; Mahvi, David M; Webster, John G. Current status of liver tumor ablation devices. Expert Review of Medical Devices 2007; Volume 4, Number 4, pp. 523-537(15)

[9] Yang D, Bertram JM, Converse MC et al. A floating sleeve antenna yields localized hepatic microwave ablation. IEEE Trans. Biomed. Eng. 2006; 53(3), 533–537.

[10] Brace CL, Laeseke PF, van der Weide DW, Lee FT Jr. Microwave ablation with a triaxial antenna: results in ex vivo bovine liver. IEEE Trans. Microw. Theory 2005; 53(1), 215–220.

[11] Longo I, Gentili GB, Cerretelli M, Tosoratti N. A coaxial antenna with miniaturized choke for minimally invasive interstitial heating. IEEE Trans. Biomed. Eng. 50(1), 82–88.

[12] Stefanie S. Jeffrey, MD; Robyn L. Birdwell, MD; Debra M. Ikeda, MD; Bruce L. Daniel, MD; Kent W. Nowels, MD; Frederick M. Dirbas, MD; Stephen M. Griffey, DVM, PhD. 1999. Radiofrequency Ablation of Breast Cancer First Report of an Emerging Technology. Arch Surg. 2003; 134:1064-1068.

[13] Jeffrey SS, Birdwell RL, Ikeda DM. Radiofrequency ablation of breast cancer: first report of an emerging technology. Arch Surg 1999; 134: 1064–8.

[14] Izzo F, Thomas R, Delrio P. Radiofrequency ablation in patients with primary breast carcinoma: a pilot study in 26 patients. Cancer 2001; 92: 2036–44.

[15] Burak WE, Agnese DM, Povoski SP. Radiofrequency ablation of invasive breast carcinoma followed by delayed surgical excision. Cancer 2003; 98: 1369–76.

[16] Hayashi AH, Silver SF, van der Westhuizen NG. Treatment of invasive breast carcinoma with ultrasound-guided radiofrequency ablation. Am J Surg 2003; 185: 429–35.

[17] Fornage BD, Sneige N, Ross MI et al. 2004. Small (≤2 cm) breast cancer treated with US-guided radiofrequency ablation: feasibility study. Radiology 2004; 231: 215–24.

[18] Marcy PY, Magne N, Castadot P, Bailet C, Namer M. Ultrasoundguided percutaneous radiofrequency ablation in elderly breast cancer patients: preliminary institutional experience. Br J Radiol 2007; 80: 267–73.

[19] Susini T, Nori J, Olivieri S et al. Radiofrequency ablation for minimally invasive treatment of breast carcinoma. A pilot study in elderly inoperable patients. Gynecol Oncol 2007; 104: 304–10.

[20] Oura S, Tamaki T, Hirai I et al. Radiofrequency ablation therapy in patients with breast cancers two centimeters or less in size. Breast Cancer 2007; 14: 48–54.

[21] Medina-Franco H, Soto-Germes S, Ulloa-Gómez JL, Romero-Trejo C, Uribe N, Ramirez-Alvarado CA, Robles-Vidal C. Radiofrequency ablation of invasive breast carcinomas: a phase II trial. Ann Surg Oncol. 2008; 15(6):1689-95.

[22] Kinoshita, T., Iwamoto, E., Tsuda, H. and Seki, K., "Radiofrequency ablation as local therapy for early breast carcinomas," 2010; Breast Cancer.

[23] Gardner RA, Vargas HI, Block JB, et al. Focused microwave phased array thermotherapy for primary breast cancer. Ann Surg Oncol 2002; 9(4):326–332.

[24] Vargas HI, Dooley WC, Gardner RA, et al. Success of sentinel lymph node mapping after breast cancer ablation with focused microwave phased array thermotherapy. Am J Surg 2003; 186(4):330–332.

[25] Vargas HI, Dooley WC, Gardner RA, et al. Focused microwave phased array thermotherapy for ablation of earlystage breast cancer: results of thermal dose escalation. Ann Surg Oncol 2004; 11(2):139–146.

[26] D. Haemmerich, L. Chachati, A.S. Wright, D.M. Mahvi, F.T. Lee Jr and J.G. Webster IEEE Trans Biomed Eng. 2003; 50 493.

[27] J. M. Bertram, D. Yang, M. C. Converse, J. G. Webster and D. M. Mahvi Biomed. Eng. Online. 2006; 5 15.

[28] S. A. Shock, K. Meredith, T. F. Warner, L. A. Sampson, A. S. Wright, T. C. Winter, III, D. M. Mahvi, J. P. Fine, and F. R. Lee, Jr Radiology 2004; 231 143.
[29] J. M. Bertram, D. Yang, M. C. Converse, J. G. Webster and D. M. Mahvi Crit. Rev. Biomed. Eng. 2006; 34 187 (2006)
[30] W.C. Dooley, H.I. Vargas, A. J. Fenn, M. B. Tomaselli and J. K. Harness Ann. Surg. Oncol. 2010; 17 1076.
[31] E. H. Wissler J. Appl. Physiol. 1998; 85 35.
[32] M. Gautherie Ann. N. Y. Acad. Sci. 1980; 335 383.
[33] Cepeda MFJ., Vera A., Leija L., Avila-Navarro, E. & Navarro, E. Coaxial Slot Antenna Design for Microwave Hyperthermia using Finite-Difference Time-Domain and Finite Element Method. The Open Nanomedicine Journal, 2011; Vol. 3, No. 1, pp. (2- 9).
[34] Cepeda MFJ. Estudio y Desarrollo de Aplicadores Coaxiales Tipo Slot de Ablación por Microondas para el Tratamiento Mínimamente Invasivo del Cáncer de Mama. PhD thesis. Centro de Investigación y de Estudios Avanzados del Instituto Politécnico Nacional; 2011.
[35] V. Ekstrand, H. Wiksell, I. Schultz, B. Sandstedt, S. Rotstein and A. Eriksson Biomed. Eng. Online. 2005; 4 41.